International Journal of Progressive Sciences and Technologies (IJPSAT)
ISSN: 2509-0119.

http://ijpsat.ijsht-journals.org
Vol. 16 No. 2 September 2019, pp. 01-13

Effect of n-Type Dopant Nitrogen in the Structure and Atomic Charges Distribution of Monolayer Graphene Sheet: A DFT Analysis

Anant Babu Marahatta[1, 2]

[1]Department of Chemistry, Amrit Science Campus, Tribhuvan University, Kathmandu, Nepal
[2]Department of Research, University Block, Southwestern State College, Kathmandu, Nepal

Abstract - Theoretical calculations are very powerful tool in the investigation of energetically most stable electronic structures and partial atomic charges distribution of the multi-atomic systems. Being one of the most important *ab initio* methods, two-dimensional (2D) periodic boundary condition (PBC) calculations of density functional theory (DFT) model are more specifically applicable while computing structures and properties of solid state multi-electron atomic or molecular systems. Present work is aimed at investigating and analyzing the effect of n-type dopant nitrogen in the ground state electronic structures and partial atomic charges distribution of the 2D monolayer graphene sheet by employing 2D PBC calculations of the DFT. At first, the 2D low energy unit cell structures of N-doped and undoped graphene sheets are produced separately and then confirmed hexagonal, honeycomb-like pattern of the carbon rings in their lattice. Interestingly, no significant distortions to the graphene lattice are observed while doping N atom (graphitic N-doping type). The inhomogeneous partial atomic charges in the terminal and nonterminal carbon atoms as well as a strong charge variation in the N and C atoms bonded to N are predicted by the Mulliken population analysis method. These theoretical achievements are not only important to speculate the most chemically "active-sites" in the N-doped and undoped monolayer graphene sheets, but also to justify increased capacitance of N-doped graphene materials. It is believed that present study would be very useful while functionalizing such 2D solid materials, means while tuning their physicochemical properties.

Keywords - 2D PBC-DFT, 2D N-doped/undoped graphene sheets, Graphitic N-doping, Unit cell geometries, and Mulliken atomic charges.

I. INTRODUCTION

In experimental research, advanced instrumentation techniques such as X−ray photoelectron spectroscopy (XPS), X-ray emission spectroscopy (XES), and Electronic Absorption and Fluorescence spectroscopy are most commonly used [1] to probe ground state electronic structures. However, in theoretical/computational research, advanced mathematical calculations such as energy minimization (also called energy or geometry optimization) techniques are used to compute the equilibrium configuration of molecules and solids. Such techniques precisely locate minimum energy confirmation from the initial structure of the molecular specimen by a series of computing process or repeated mathematical calculations [2]. This computational procedure involves calculation of the wave function and energy at a starting molecular confirmation and then proceeding to search the nearest minimum energy confirmation using the smallest number of calculations possible. Thus, in computational/ theoretical chemistry, the energy minimization methodology that generates atomic Cartesian coordinates of the most stable electronic structure of the molecule, dimensions of the optimized parameters such as atomic distances and angles, Mulliken atomic charges distribution, and electric dipole moments [3] is widely used to find a route from a trial structure to the global minimum structure (ground state electronic structure). In order to implement such powerful

Corresponding Author: Anant Babu Marahatta

computational methodology in the theoretical research, an electronic structure package known as *Gaussian* has been offering the wide verities of computational models [4]. A density functional theory (hereafter, DFT) model is one of them. It is a renowned quantum mechanical model for investigating ground state electronic structures of the multi-electron atomic or molecular systems [5, 6] in spite of its many notable limitations while applying to large molecular/atomic assemblies [7]. Even though it includes a formalism for approximately solving Schrodinger's wave equation, it produces better results than *ab initio* electronic structure methods at the similar computational cost [8, 9]. It offers very promising calculations that are applicable to optimize solid state systems: one-dimensional, two-dimensional (hereafter, 2D), and three-dimensional periodic boundary condition (hereafter, PBC) calculations for analytic energy and optimizations, and numerical frequencies [3].

As the 2D monolayer graphene sheet possesses many extraordinary properties in terms of strength (200×stronger than steel), electrons mobility (100×faster than silicon), electricity (13×better than copper), and heat conduction (2×better than diamond) [10-16], attaching foreign atoms and functional parts in its lattice atoms and/or substituting lattice atoms by some foreign elements may lead to modify many of these properties, resulting derivation of many types of functional graphene nanostructures and technologically relevant solid substrates. A process of adding/substituting some impurity atoms in the pure graphene structure is called doping and the impurity atoms are called dopants [17]. Among the various possible n-type (electron donor atoms) and p-type (electron acceptor atoms) dopants, the n-type dopant nitrogen (hereafter, N) being its atomic radius (A_r) comparable to that of carbon (A_r of C and N are 67 pm and 56 pm respectively) has captivated many researchers as its doping directly affects many physicochemical properties of the monolayer graphene [17] sheet without changing original hexagonal lattice structure [10-13] and thickness (= 0.335 nm) [14-16] in the 2D plane. In the N doping process, three possible types of C−N bonding configurations are found in the literatures: graphitic N, pyridinic N, and pyrrolic N [17-19]. Among them, the graphitic N-doping type that can be achieved simply by substituting graphene ring C by N atom has been considered in this study. Because of such substitutional doping of C by N, the atomic charges distribution in the entire graphene framework would be highly influenced (electronegativity (χ) values for C and N by Pauling scale are 2.55 and 3.04, respectively) whereas, a high electron mobility of the original graphene may remain preserved [19]. Several experimental investigations of the nitrogen doped (hereafter, N-doped) graphene based materials have claimed their potential applications in the field of fuel cells (as a catalyst or carbon supports), catalytic chemistry including industrial catalytic reactions (oxygen reduction reaction (ORR), other catalysts supporter), and technology development by fabricating many types of metal-free carbon-based catalysts [18-23].

On the one hand, N-doped graphene possesses very impressive characteristics that not only enable it to show many exceptional properties such as its high electrochemical activity towards ORR, higher stability and durability than Pt-based catalysts, and high conductivity, but also make it an emerging nanomaterial for developing many hybrid materials for energy applications (in solar cell) [24], but on the other hand, in-depth investigation about what makes it such an amazing material carrying more potentialities than undoped graphene is still lacking. In particular, comparatively better theoretical/computational methodologies that can be used to determine the effect of n-type nitrogen dopant in the ground state electronic structure and Mulliken atomic charges distribution of the monolayer graphene sheet are being widely sought. In this context, the 2D PBC calculations of DFT that are previously found to produce very reliable results while applying to pure 2D monolayer graphene sheet [25] are applied again to its N-doped counterpart and presented the theoretical results. Previously, the DFT predicted geometries and Mulliken charges distribution of the 2D monolayer graphene sheet were explained straight forward [25] rather than comparing with its N-doped counterpart. That is why, the proper comparative studies of the ground state electronic structures and atomic charges distribution before and after doping carbon by N in the graphene lattice are quite indispensable. For this purpose, few data sets and figures from the previous publication are reproduced here. It is believed that present theoretical studies have unveiled an extensive knowledge for explaining the effects of n-type dopant nitrogen in modifying many physicochemical properties of such 'wonder carbon material'. The structure of this paper is as follows. The computational methods are outlined in section 2. The results and discussion are presented in section 3 and the summary and conclusions are given in section 4.

II. COMPUTATIONAL METHODS

At first, a trial structure of the undoped monolayer graphene sheet with 18 carbon atoms and 14 dummy atoms in two lattice dimension was built by using GaussView visualization application software [26] and then one of the

central ring carbon atoms was substituted by nitrogen (graphitic N-doping) to build N-doped monolayer graphene sheet as shown in chart 1. These initial unit cell structures of the N-doped and undoped monolayer graphene have each C−C (and a C-N) bond length 1.4113Å, each C−C−C (or C−N−C) bond angle 119.973°, and two sets of C−C−C−C dihedral angles: C3−C15−C7−C16 (N18−C14−C6−C15 in N-doped graphene) type = 0°, and C15−C7−C16−C8 (C14−C6−C15−C7 in N-doped graphene) type = 180°.

Chart 1 **Trial structures of (a) N-doped, and (b) undoped monolayer graphene sheet. The central carbon ring is encircled.**

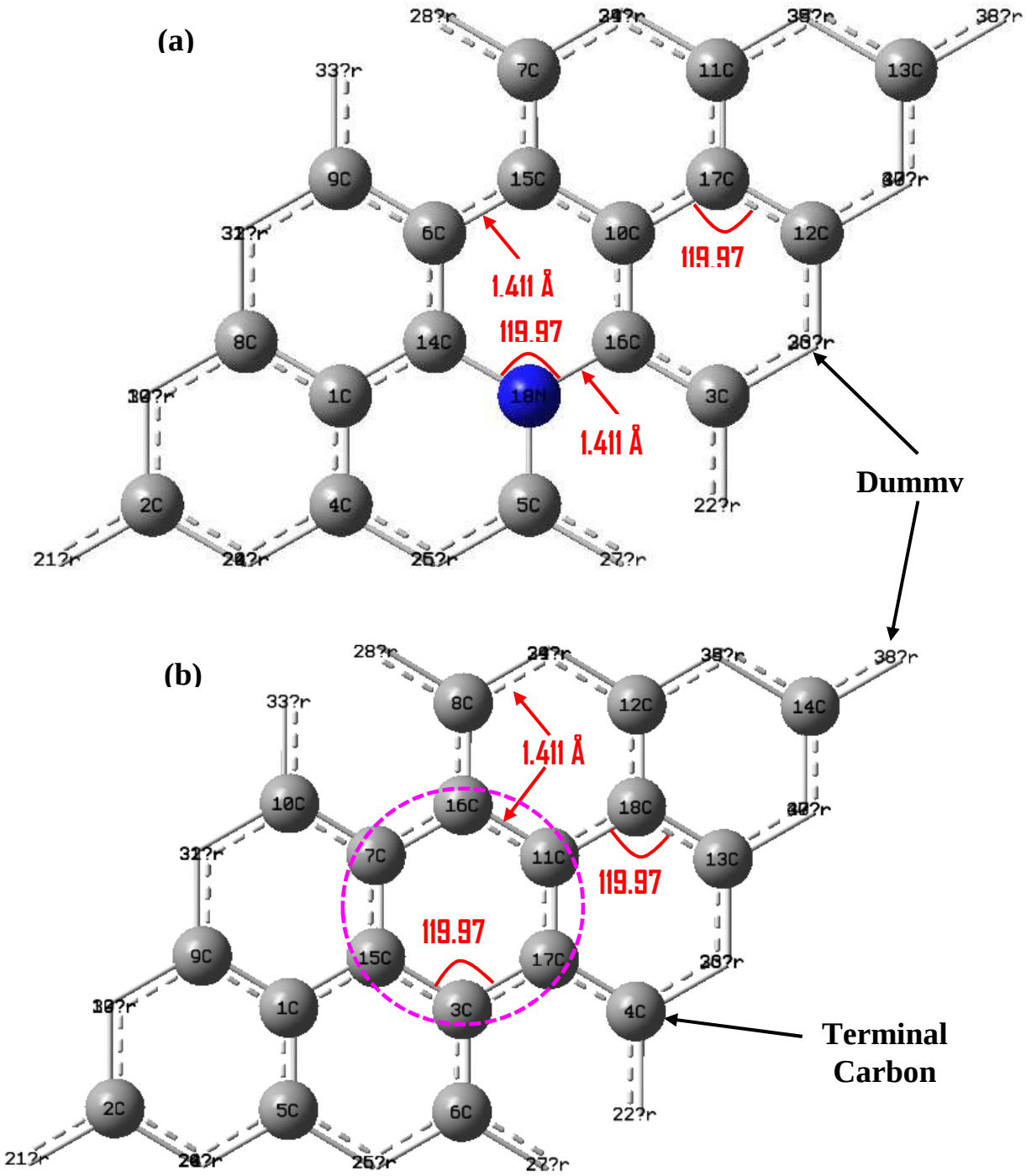

The edge or terminal carbon atoms were left as an incomplete bonding in order to realize the original graphene sheet computationally. The initial atomic Cartesian coordinates were extracted from each trial structure and used them manually to prepare *Gaussian* input files separately for their geometry optimization. All the Gaussian keywords and methodologies were selected as instructed in *Gaussian* 09 manual [3]. The hybrid functional based DFT method known as B3LYP was used with the basis set of this type: 3−21G i.e. the methodology used was DFT: B3LYP/3−21G; the periodic systems were specified with a normal trial molecule specification for the unit cell; and the additional two translational vectors (hereafter, TVs) were appended to each molecule specification with no intervening blank line. By utilizing such TVs, the DFT method was forced to replicate the unit cell in the specific direction(s) and hence, created a supercell. In this way, the 2D PBC calculations in B3LYP/3−21G were set for approximating an infinite 2D solid state N-doped and undoped graphene system separately. Moreover, to solve the electronic Schrodinger equation iteratively, the self-consistent field (SCF) with both default SCF procedure (SCF=Tight) and Berny algorithm for optimizations to a local minimum were selected in *Gaussian* 09 [4]. The *Gaussian* output log file was read by using the *Gaussian* graphical interface i.e. GaussView and various chemical data displayed in three dimensions were extracted. And then the optimized structures, optimized parameters such as bond lengths, bond angles, and torsional angles, and Mulliken atomic charges distribution of the both N-doped and undoped monolayer graphene sheet were analyzed thoroughly.

III. RESULTS AND DISCUSSION

3.1 Ground state electronic structures

A DFT optimized geometries of the N-doped and undoped monolayer graphene sheets are shown in Figure 1 where the grey and blue spheroids represent C and N atoms and the x-axis and y-axis represents the first two dimensions and the z-axis, a third dimension. For analyzing the optimized geometry and partial atomic charges distribution more clearly, all the atoms present in the both graphene structures are leveled as 1C, 2C, 3C, etc. By looking at the optimized structures carefully, one can confirm that both N-doped and undoped monolayer graphene sheets that are composed entirely of single layer of carbon atoms have hexagonal, honeycomb-like pattern of carbon rings. Interestingly, no significant structural changes in the carbon motif of the undoped graphene sheet is observed while substituting 3C by 18N (graphitic N-doping). The optimized unit cell structures of both graphene sheets viewed through z-axis (Figure 1) and xy plane (Figure 2) demonstrate that both of them consist of only two dimensions: length and width represented in x- y coordinate axis. As a rule, the optimized geometries must be specified mostly in terms of the three parameters namely bond length: an average distance between the nuclei of two atoms bonded together in any given molecule; bond angle: angle formed between three atoms across the two bonds; and torsional angle: angle between the plane formed by the first three atoms and the plane formed by the last three atoms, the explicitly measured theoretically calculated values of them for N-doped and undoped monolayer graphene sheets are listed in Table 1 and Table 2 respectively.

If the bond angles and lattice structures of the graphene sheets are compared before and after doping N, slight angular distortions resulting a relatively small distortion on the graphene lattice are observed. Such negligible angular distortions might be due to bonding between C and N having dissimilar types of hybridized orbitals with different angular orientation: C has sp^2 hybridized orbitals (angular orientation: 120°) and N has sp^3 hybridized orbitals (angular orientation: 107° due to lone pair-bond pair repulsion). As a whole, all the concerned C−N and C−C bond lengths and the C−N−C and C−C−C bond angles in the optimized unit cells of N-doped and undoped monolayer graphene sheets are found to be in the range of 1.45 Å and 1.44 Å (Trial structure: C−N or C−C bond length = 1.411 Å), and 119.5° and 120° (Trial structure: C−N−C or C−C−C bond angle = 119.97°) respectively, and the dihedral angles are either 0° or 180° (depending on the plane formed by the atoms) as in the specific trial structures (chart 1). Such DFT computed values of the optimized unit cells parameters are found to be consistent with the experimentally determined and dynamically simulated values: i) for N-doped graphene layer: experimental C−N and C−C bond lengths are 1.41Å and 1.42 Å respectively [27] and Vienna *ab initio* simulation package (VASP) calculated values: C−N−C bond angle = 118°, C−C−C bond angle = 120° [28] and ii) for undoped graphene layer: experimental C−C bond length = 1.42Å, and C−C−C bond angle = 120° [29] and dynamically simulated (molecular dynamics simulation) values: C−C bond length = 1.418 Å, and C−C−C bond angle = 120° [30]. As in experiments and simulations, present DFT computed C−N and C−C bond lengths (1.45 Å and 1.44 Å respectively) of the N-doped and undoped graphene layers are found to be intermediate while comparing it with the lengths of a C=C double bond (1.35 Å) in ethene ($H_2C=CH_2$) and a C−C

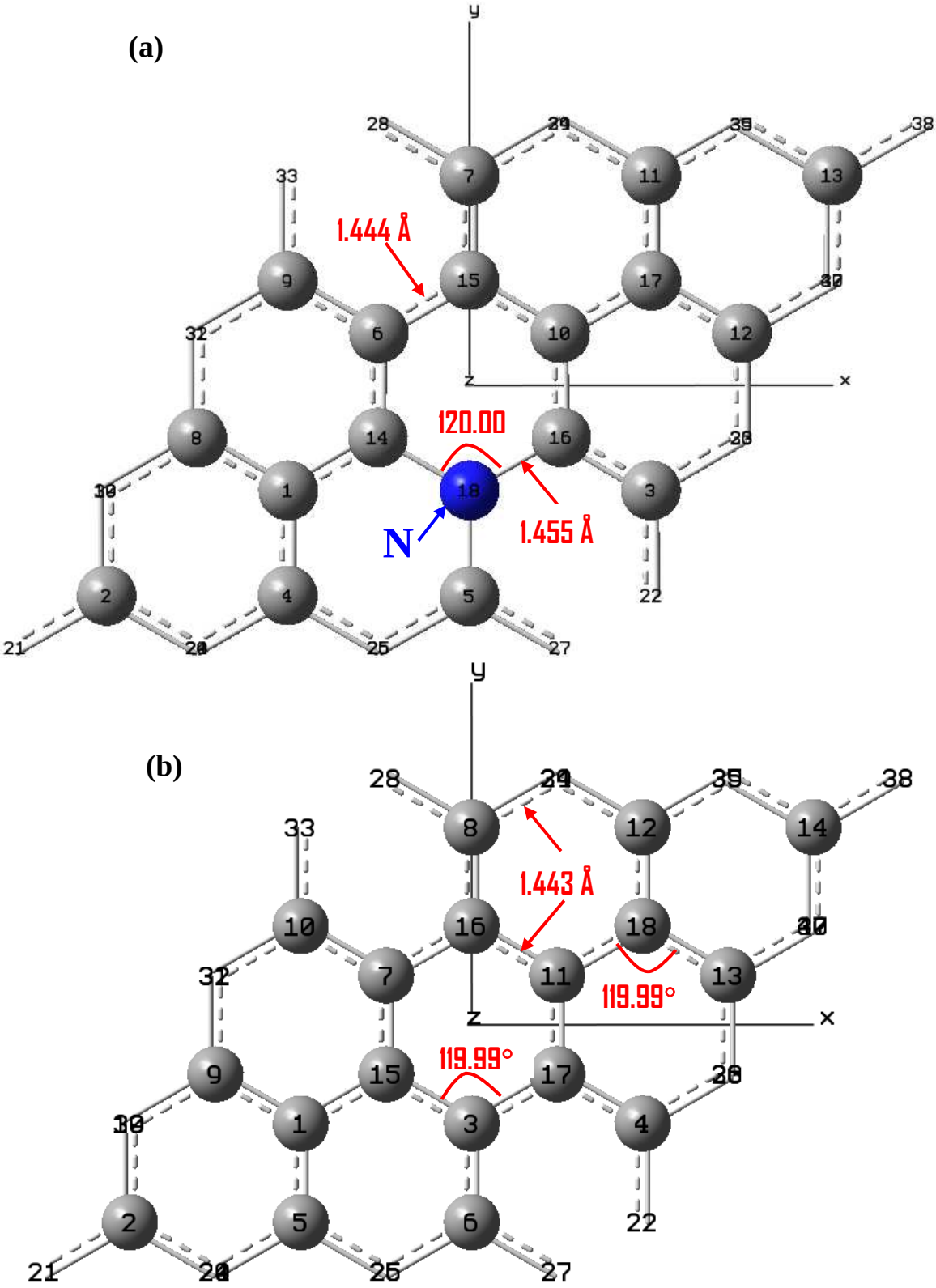

Figure 1. DFT optimized unit cell geometries of (a) N-doped, and (b) undoped monolayer graphene sheet viewed through z-axis. The grey and blue spheroids represent C and N atoms, respectively.

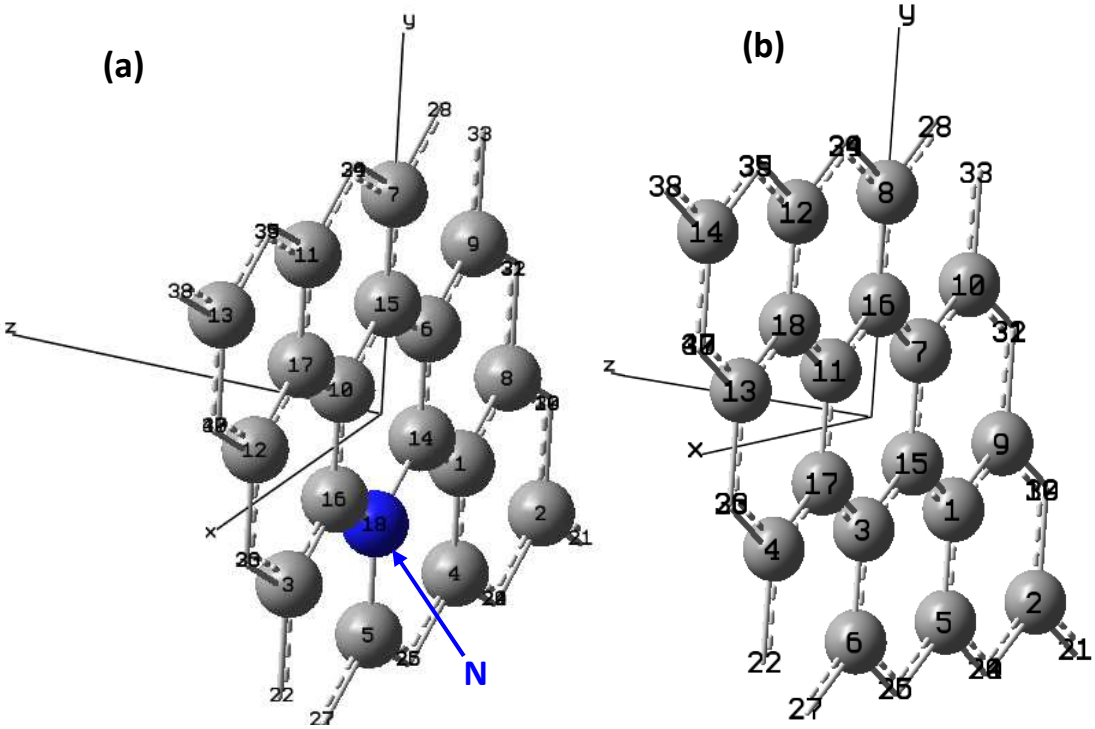

Figure 2. DFT optimized unit cell geometries of (a) N-doped and (b) undoped monolayer graphene sheet viewed through xy plane. The grey and blue spheroids represent C and N atoms, respectively.

Table 1. DFT optimized parameters of the N-doped monolayer graphene sheet

Bond length (Å)	**Bond angle (°)**	**Dihedral angle (°)**
C1-C4 = 1.4439	C4-C1-C8 = 119.78	C4-C1-C14-C6 = 180.00
C1-C8 = 1.4463	C4-C1-C14 = 120.82	C8-C1-C14-N18 = 180.00
C1-C14 = 1.4323	C8-C1-C14 = 119.41	C5-N18-C14-C6 = 180.00
C3-C16 = 1.4320	C9-C6-C14 = 119.40	C14-N18-C16-C3 = 180.00
C3-C22 = 1.4439	C9-C6-C15 = 119.79	C16-C10-C17-C11 =180.00
C3-C23 = 1.4464	C14-C6-C15 = 120.81	C14-C6-C15-C7 = 180.00
C5-N18 = 1.4557	C3-C17-C4 = 120.03	C4-C1-C14-N18 = 0.00
C6-C9 = 1.4463	C15-C10-C16 = 120.84	C8-C1-C14-C6 = 0.00
C6-C14 = 1.4323	C15-C10-C17 = 119.78	C1-C14-C6-C9 = 0.00
C6-C15 = 1.444	C16-C10-C17 = 119.38	C3-C16-C10-C17 = 0.00
C7-C15 = 1.4378	C1-C14-C6 = 121.08	C10-C16-C18-C14 = 0.00
C10-C15 = 1.4435	C1-C14-N18 = 119.46	C11-C17-C10-C15 = 0.00
C10-C16 = 1.4325	C6-C15-C7 = 120.26	C17-C10-C15-C7 = 0.00
C10-C17 = 1.4464	C6-C15-C10 = 119.45	C16-C10-C15-C7 = −180.00
C11-C17 = 1.4464	C7-C15-C10 = 120.29	N18-C14-C6-C9 = −180.00
C12-C17 = 1.4384	C3-C16-C10 = 121.11	C3-C16-C10-C15 = −180.00
C14-N18 = 1.4553	C3-C16-N18 = 119.46	C4-C1-C14-C6 = −180.00
C16-N18 = 1.4558	C10-C16-N18 = 119.44	C1-C14-N18-C16 = −180.00
etc.	C5-N18-C14 = 120.00	**etc.**
	C5-N18-C16 = 119.99	

	C14-N18-C16 = 120.00 **etc.**	

Table 2. DFT optimized parameters of the undoped monolayer graphene sheet

Bond length (Å)	**Bond angle (°)**	**Dihedral angle (°)**
C1-C9 = 1.44359 C1-C5 = 1.44383 C1-C15 = 1.44324 C15-C7 = 1.44392 C15-C3 = 1.44374 C3-C6 = 1.44317 C7-C10 = 1.44303 C7-C16 = 1.44383 C16-C11 = 1.44387 C11-C17 = 1.4404 C17-C4 = 1.44280 C11-C18 = 1.44280 C12-C18 = 1.44413 C18-C13 = 1.44387 C8-C28 = 1.44416 C5-C25 = 1.44309 **etc.**	C9-C1-C5 = 120.01 C15-C1-C5 = 119.99 C15-C1-C9 = 119.99 C10-C7-C15 = 120.01 C15-C3-C6 = 120.01 C6-C3-C17 = 120.01 C3-C17-C4 = 120.03 C3-C17-C11 = 119.99 C17-C11-C16 = 120.03 C11-C16-C7 = 119.99 C16-C8-C29 = 120.04 C16-C11-C18 = 119.99 C12-C18-C13 = 119.96 C18-C13-C30 = 119.99 C18-C13-C29 = 120.04 C16-C7-C10 = 120.01 **etc.**	C5-C1-C15-C3 = 0.00 C5-C1-C15-C7 = 180.00 C6-C3-C15-C7 = 180.00 C6-C3-C17-C4 = 0.00 C4-C17-C11-C16 = 180.00 C4-C17-C11-C18 = 0.00 C17-C11-C18-C13 = 0.00 C12-C18-C11-C16 = 0.00 C8-C16-C7-C10 = 0.00 C38-C14-C35-C12 =180.00 C25-C5-C20-C2 = 180.00 **etc.**

single bond (1.47 Å) in ethane (H_3C-CH_3). It reflects that each C−N and C−C bond in the N-doped and undoped graphene rings has partial double bond character, means the electrons inside the graphene rings are not associated with any single atom or single covalent bond but are likely to be found equally anywhere along the chemical bonds as in other aromatic conjugated π electron systems such as benzene etc. Such resonating behavior of electrons is most commonly called electrons delocalization. In order to accurately depict the nature of bonding and the electrons resonance, the carbon rings (with and without N atom) of both of the graphene sheets are shown with a conjugated double bonds in Figure 1. The genius of the electrons delocalization model can be further explained by both hybridization and valence bond theory (hereafter, VBT) concepts. As each interior and exterior C−C−C and C−N−C bond angles of the DFT optimized graphene carbon rings in both N-doped and undoped graphene layer are measured as ~120° which is almost equal to C−C−C bond angle in its graphite structure and in its aromatic conjugated π electron system (benzene ring) but slightly larger than the prospective value of 109.5° in its diamond structure, these three C−C−C and C−N−C atoms must be bonded to each other by forming trigonal units with no angular strain at all (i.e. bond angle = ~120°), which then unite together and produce a regular hexagonal shape of the graphene rings as shown in Figure 1. According to the VBT, such regular hexagonal shape of the carbon rings (with and without N atom) will only be formed whenever each carbon atom (C: $1S^2$, $2S^22P^2$) has $3sp^2$ hybrid orbitals bonded covalently to three other carbon (each nitrogen atom (N: $1S^2$, $2S^22P^3$) has $3sp^3$ hybrid orbitals bonded covalently to three other carbon atoms in the case of N-doped graphene) atoms (*pi* (π) bond) on the 2D plane and the remaining each non-bonding half-filled and full-filled orbital of C and N atoms respectively on the third dimension. It means, each carbon and nitrogen atom has one and two electrons leftover (i.e. non-bonding electrons) on the third dimension respectively. So, the giant carbon network of the graphene sheet contains many free electrons (π electrons) which may form electron cloud spreading above and below the graphene sheet. In the case of N-doped graphene sheet, the lone pair (two non-bonding electrons) of each N may conjugate with this π electron cloud of the carbon network resulting huge modification of the graphene physical and chemical properties. This is one of the reasons why N-doped and undoped monolayer

graphene sheets show remarkable electrical and heat conductivity. In addition to this, the additional mobile electrons provided by the nitrogen atom to the graphene π electron cloud (that is why, N atom is an n-type dopant) may be responsible for: increased capacitance of an N-doped graphene (~7 times higher than graphene oxide GO), its behavior as an N-type semiconductor and electric double layer capacitor (EDLC) [31].

3.2 Mulliken population analysis

A Mulliken population analysis [32] is the cheapest but fastest way to compute Mulliken atomic charges theoretically even though it tends to produce qualitative results at best. Such atomic charges can be used to characterize the electronic charges distribution in a molecule. More specifically, they are very useful to estimate the partial atomic charges qualitatively. The DFT computed Mulliken charges distribution in the nitrogen and carbon atoms of the N-doped and undoped monolayer graphene sheets can be observed directly by the color of the spheroids in Figure 3 (color index and range are given), where the most red colored (N18 in Figure 3a, C2 in Figure 3b), and the most green colored (C14, C16, C5 in Figure 3a and C6 in Figure 3b) spheroids represent the most negatively and the most positively charged carbon atoms respectively; the second most red colored (C14 in Figure 3b) and the second most green colored (C4, C8, and C10 in Figure 3b) spheroids represent the second most negatively and the second most positively charged carbon atoms respectively; the most black colored (C8, and C17 in Figure 3a and C12, C13, C15, C9, and C5 in Figure 3b) and the dark purple colored (C1, C2, C3, C4, C6, C7, C10, C11, C12, C13, and C15 in Figure 3a and C7, and C3 in Figure 3b) spheroids represent almost neutral and the least negatively charged carbon atoms (neglecting -0.000 range) respectively. The numeral values of Mulliken atomic charges in the N-doped and undoped monolayer graphene sheets are listed in Table 3 and Table 4 respectively, where atom numbers are assigned in accordance with Figure 3.

Table 3. Mulliken charge distribution in the N-doped monolayer graphene sheet *

Atom numbers	Charge	Atom numbers	Charge
1	-0.008	10	-0.008
2	-0.008	11	-0.008
3	-0.008	12	-0.006
4	-0.007	13	-0.008
5	0.085	14	0.085
6	-0.008	15	-0.007
7	-0.005	16	0.085
8	0.001	17	0.001
9	0.001	18(N)	-0.180

*atom numbers are in accordance with Mulliken Charge distribution shown in Figure 3(a).

Table 4. Mulliken charge distribution in the undoped monolayer graphene sheet *

Atom numbers				Charge	Atom numbers	Charge
1				-0.000	10	0.002
2				-0.004	11	-0.000
3				-0.001	12	0.000
4				0.002	13	0.000
5				0.000	14	-0.003
6	0.003	15	0.000			
7	-0.001	16	-0.000			
8	0.002	17	-0.000			
9	0.000	18	-0.000			

* atom numbers are in accordance with Mulliken Charge distribution shown in Figure 3(b).

By carefully analyzing these charge distributions in both types of graphene layers, one can find that: (i) in N-doped graphene layer: partial atomic charges of the terminal carbon atoms represented by black and dark purple spheroids in Figure 3a differ in wide range from those of the nitrogen (represented by red colored spheroid) and nitrogen-bonded carbon atoms (represented by green colored spheroids) and (ii) in undoped graphene layer: partial atomic charges of the terminal carbon atoms (represented by red and green colored spheroids in Figure 3(b)) differ in wide range from those of the non-terminal and central atoms (represented by black and dark purple spheroids in Figure 3(b)). In the case of N-doped graphene, such inhomogeneous charge distribution is arose due to a strong ability of nitrogen atom to attract shared electrons in a covalent bond with carbon atoms as electronegativity of nitrogen (χ_N = 3.04) is greater than that of carbon (χ_C = 2.55). Such effect is much more pronounced in the nitrogen bonded carbon atoms (green colored spheroids C5, C14, and C16) as observed in Figure 3(a) where they bear maximum partial positive atomic charges (Mulliken charge unit: +0.085, 85 times less in electron density than the second highest positively charged carbon atoms C8, C9, and C17) as listed in Table 3. This is the reason why nitrogen bonded carbon atoms (C5, C14, and C16 in the unit cell and their replicates in the super cell lattice structure) behave as the most "active-sites" for hosting many types of chemical reactions including oxygen reduction reaction (hereafter, ORR) for activating O_2 and covalent alkylation reaction for deriving many types of N-doped graphene materials by varying the band gap between frontier orbitals. Such effect of n-type dopant N estimated by the DFT model would be a strong supporting evidence for claiming N-doped graphene material as metal free electro catalyst for efficient ORR in fuel cells and covalently functionalizable material. Similar type of excessive partial positive atomic charges development in the nitrogen bonded carbon atoms and their strong tendencies towards chemical reactivity are confirmed by the FTIR and XPS valence band spectra [33]. Those electron deficient carbon atoms (Lewis acids) pointed out by the DFT calculations may also behave as "Lewis basic sites" because Lewis base type anionic radicals such as OH^-, CN^-, O^{2-}, ROH, RO^-, $RCOO^-$, H_2N^- and many other nucleophiles can easily be attached to them via electron-pair donor-acceptor bonding scheme. This would be a very promising and potential characteristic feature for the N-doped monolayer graphene sheet as it allows us to functionalize this material according to our need. Again, the DFT predicted excessive accumulation of partial negative charges on the nitrogen atom (Mulliken charge unit is: -0.180 (Table 3), 22.5 times more in electron density than in the second highest negatively charged carbon atoms: C1, C2, C3, C6, and C13) has made the N-doped graphene as atomically sharp point impurity containing material. It further illustrates that a dopant 'N atom' in the graphene lattice can serve as an electron donor (n-type dopant N) and after losing an electron, it may act as a positively charged scattering center for electron transport chain and hence, may exhibit an electron-hole asymmetry (a key to superconductivity) in transport phenomena. These sort of applicable consequences are also confirmed experimentally by Li *et al.* while measuring electrical and magneto transport properties [34] of graphitic N-doping type graphene materials. Therefore, the ability to tailor N-doped monolayer and multilayer graphene sheets with different percentage composition of n-type dopant N and to tune its environment inside their lattice may allow one to control over device sensitivity in future.

As both types of graphene layers are 2D network of carbon (and nitrogen) atoms bound to one another by covalent bonds, the terminal atoms obviously miss some C−C bonds unlike by the non-terminal and central atoms, resulting the difference in their charges. The same charge inhomogeneity in the graphene terminals and edges has been observed experimentally by the scanning gate microscopy [35]. Moreover, the central carbon atoms of the graphene sheet which form three covalent bonds with the three neighboring carbon atoms (two neighboring carbon and one nitrogen atoms in N-doped graphene) are found to possess least or almost no charge (Table 3 and Table 4). This can be explained simply by calculating formal charge of an atom: Formal atomic charge = number of valence electrons − $[(\frac{1}{2}\times$ number of bonding electrons$)$ + number of non-bonding electrons$]$. To make it easier, the formal atomic charge of the carbon atoms not bonded to nitrogen atom in the central graphene ring encircled in Figure 3 is calculated as: Formal atomic charge of carbon $= 4 - [(\frac{1}{2}\times 6) + 1] = 0$. This should not be the case for the terminal carbon atoms because they have less number of bonding electrons due to missing some C−C bonds, and whenever they are made saturated with hydrogen atoms, more stabilization occur as reported earlier by Y. Miyamoto *et al.* [36] and then only they may behave like central carbon atoms in terms of their formal atomic charges. However, the tunneling electron microscopy revealed that the graphene sheet with unsaturated terminal carbon atoms forms triple bonds itself (as in central carbon) along the edges and terminals under vacuum and attains self-stability [37]. If so, the terminal carbon atoms of the monolayer graphene sheet

under vacuum should also possess formal atomic charge zero. These contradictory observations are still under scientific consideration.

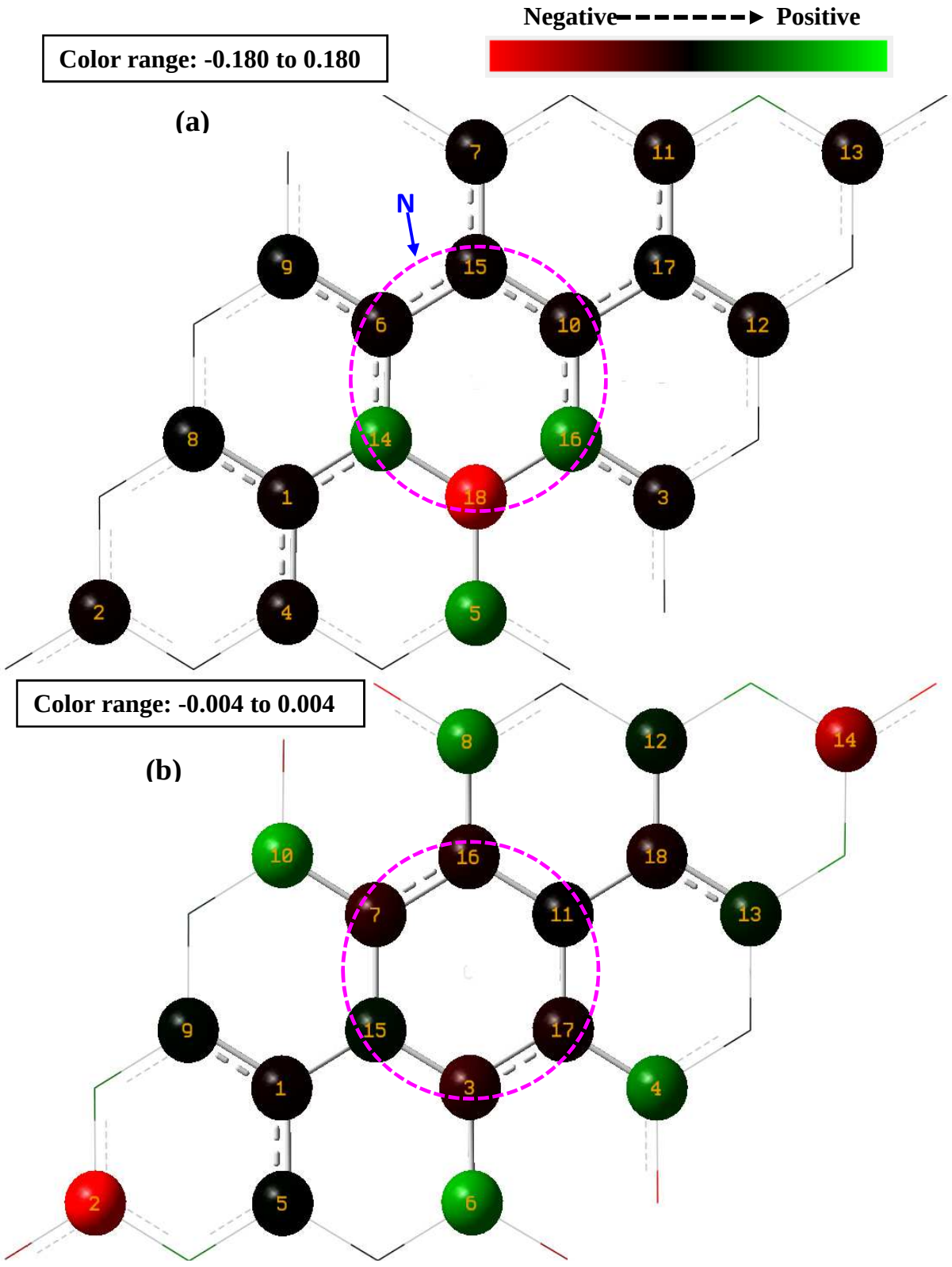

Figure 3. Mulliken charges distribution in DFT optimized unit cell geometries of (a) N-doped, and (b) undoped monolayer graphene sheet. The central graphene rings are encircled.

Even though, the absolute magnitude of the atomic charges computed by the Mulliken populations analysis displays a high degree of sensitivity to the types of basis set used, the qualitative results of them that are produced by DFT:B3LYP/3−21G method were presented here. In future studies, analyses of the natural bond orbital (NBO) [38] and electron density surfaces of the frontier molecular orbitals can be performed for more accurate distribution of the charges.

IV. Conclusion

At present, the effect of n-type dopant nitrogen in the ground state electronic structures and Mulliken charges distribution of the two dimensional (2D) monolayer graphene sheet are investigated by the density functional theory (DFT) model. Even though it is computationally cheap quantum mechanical model compare to ab initio, it has shown exceptional skills to unveil an extensive knowledge for interpreting ground state electronic structures and partial atomic charges distribution while doping a nitrogen atom in the pure graphene lattice. The energetically most stable ground state electronic structures of the N-doped and undoped monolayer graphene sheets produced by the DFT: B3LYP/3−21G methodology under 2D periodic boundary condition (PBC) have depicted their hexagonal, honeycomb-like pattern of the carbon rings with or without substitutional nitrogen atom respectively. Interestingly, no significant structural changes in the carbon motif of the graphene sheet is observed while doping a nitrogen atom of type graphitic N-doping except slight reasonable angular distortions. The DFT computed dimensions of the bond lengths, bond angles, and torsional angles for these two optimized unit cell geometries are found in close consistence to each other. In turn, they are found to be in good agreement with the concerned experimental, molecular dynamics, and Vienna ab initio (VASP) simulated values. Moreover, the intermediate length of C−N (1.45 Å) and C−C (1.44 Å) bonds measured in the respective DFT optimized unit cell structure has elucidated their conjugate double bond characters. The Mulliken population analysis method of electronic charge distribution has predicted unequal partial atomic charges in the terminal and non-terminal/central carbon atoms of both types of the graphene sheet, as observed experimentally. Additionally, the DFT determined huge charge inhomogeneity in nitrogen and nitrogen bonded carbon atoms of the N-doped graphene sheet has not only speculated its most "active-sites" or "Lewis basic sites" (electron deficient carbon atoms) for hosting many chemical reactions such as oxygen reduction (ORR), covalent alkylation, and nucleophilic additions, but also supported its enhanced capacitance and conductivity. Thus, the present theoretical calculations revealed at least few conspicuous facts for justifying the effect of n-type dopant while doping in the 2D monolayer graphene lattice. As all the theoretically calculated results achieved here are as reliable as experimental results, the DFT skills for computing ground state electronic structures and partial atomic charges distribution for the 2D N-doped and undoped graphene-based materials are regarded as outstanding. The similar type of computational methodology can be adopted to other n-type dopants: Si-doped, S-doped, P-doped, and N-, P- and S- tridoped monolayer graphene as well to p-type dopants: B-doped monolayer graphene.

References

[1] Khyzhun, Y., Strunskus, T., Cramm, S., & Solonin, Yu. M. (2005). Electronic structure of $CuWO_4$: XPS, XES and NEXAFS studies. *Journal of Alloys and Compounds*, 389:14-20.

[2] Daudel, R. (1966). Electronic Structure of Molecules, Elsevier publication.

[3] Gaussian 09 manual. *http://gaussian.com/geom/?tabid=1#GeomkeywordReadOptim izeoption*

[4] Frisch, M. J., Trucks, G. W., Schlegel, H. B., Scuseria, G. E., Robb, M. A., Cheeseman, J. R., Scalmani, G., Barone, V., Petersson, G. A. , & Nakatsuji H., *et al.* (2004). Gaussian 09, Revision C.01, Gaussian, Inc.

[5] Madan, R. D. (1997). Modern Inorganic Chemistry, S. Chand & Company.

[6] McQuarrie, D. A., & Simon, J. D. (1998). Physical Chemistry: Molecular Approach, Viva Books.

[7] Cohen, A. J., Sánchez, P. M., & Yang, W. (2008). Insights into Current Limitations of Density Functional Theory. *Science* 321:792-794.

[8] Hohenberg, P., & Kohn, W. (1964). Inhomogeneous Electron Gas. *Physical Review B* 136: 864-871.

[9] Kohn, W., & Sham, L. J. (1965) Self-Consistent Equations Including Exchange and Correlation Effects. Physical Review 140:A1133.

[10] Shtepliuk, I., Caffrey, N. M., Iakimov, T., Khranovskyy, V., Abrikosov, I. A. & Yakimova, R. (2017). On the interaction of toxic heavy metals (Cd, Hg, Pb) with graphene quantum dots and infinite graphene. *Scientific Report* 7:3934–3950.

[11] Tachikawa, H., Iyama, T., & Kawabata, H. (2014). Effect of hydrogenation on the band gap of graphene nano-flakes. *Thin Solid Films* 554:199-203.

[12] Anota, E. C., Juarez, A. R., Castro, M., & Cocoletzi, H. H. (2013). A density functional theory analysis for the

adsorption of the amine group on graphene and boron nitride nanosheets. *Journal of molecular modeling* 19:321-328.

[13] Graphene: The Carbon-Based 'Wonder Material'. *https://www.compoundchem.com/ 2015 /06/23/ graphene/*

[14] Kelly, B. T. (1981). Physics of Graphite, Applied Science: London.

[15] Dresselhaus, M. S., Dresselhaus, G., & Eklund, P. C. (1996). Science of Fullerenes and Carbon Nanotubes, Academic Press: San Diego.

[16] Ni, Z. H., Wang, H. M., Kasim, J., Fan, H. M., Yu, T., Wu, Y. H., Feng, Y. P., & Shen, Z. X. (2007). Graphene Thickness Determination Using Reflection and Contrast Spectroscopy. *Nano Letters* 7:2758-2763.

[17] Bundaleska, N., Henriques, J., Abrashev, M., Botelho do Rego, A. M., Ferraria, A. M., Almeida, A., Dias, F. M., Valcheva, E., Arnaudov, B., Upadhyay, K. K., Montemor, M. F., & Tatarova, E. (2018). Large-scale synthesis of free-standing N-doped graphene using microwave plasma, *Scientific Reports* 8:12595:1-10.

[18] Tatarova, E., Bundaleska, N., Sarrette, J. Ph & Ferreira, C. M. (2014). Plasmas for environmental Issues: from hydrogen production to 2D materials assembly. *Plasma Sources Science and Technology* 23:063002.

[19] Wang, X., Sun, G., Routh, P., Kim, D. H., Huang, W., & Chen, P. (2014). Heteroatom-doped graphene materials: syntheses, properties and applications. *Chemical Society Reviews* 43:7067-7098.

[20] Wang, H., Maialagan, T. & Wang, X. (2012). Review on recent progress in nitrogen-doped graphene: synthesis, characterization, and its potential applications. *ACS Catalysis* 2:781–794.

[21] Jafri, R. I., Rajalakshmi, N. & Ramaprabhu, S. (2010). Nitrogen doped graphene nanoplatelets as catalyst support for oxygen reduction reaction in proton exchange membrane fuel cell. *Journal of Materials Chemistry* 20:7114–7117.

[22] Shao, Y., Zhang, S., Engelhard, M. H., Li, G., Shao, G., Wang, Y., Liu, J., Aksay, I. A., & Lin, Y. (2010). Nitrogen-doped graphene and its electrochemical applications. *Journal of Materials Chemistry* 20:7491–7496.

[23] Du, D., Li, P. & Ouyang, J. (2015). Nitrogen-doped reduced graphene oxide prepared by simultaneous thermal reduction and nitrogen doping of graphene oxide in air and its application as an electrocatalyst. *ACS Applied Materials & Interfaces* 7:26952–26958.

[24] Barrejón, M., Arellano, L. M., Gobeze, H. B., Gómez-Escalonilla M. J., Fierro, J. L. G., D'Souza, F., & Langa, F. (2018). N-Doped graphene/C_{60} covalent hybrid as a new material for energy harvesting applications. *Chemical Science* 9:8221-8227.

[25] Marahatta, A. B. (2019). A DFT Analysis for the Electronic Structure, Mulliken Charges Distribution and Frontier Molecular Orbitals of Monolayer Graphene Sheet. *International Journal of Progressive Sciences and Technologies* 16(1):51-65.

[26] Frisch, Æ., Hratchian, H. P., Dennington II, R. D., Keith, T. A., & Millam,J. (2009). Gauss view 5 Reference, Gaussian, Inc.

[27] Xing, Z., Ju, Z., Zhao, Y., Wan, J., Zhu, Y., Qiang, Y., & Qian Y. (2016). One-pot hydrothermal synthesis of Nitrogen-doped graphene as high-performance anode materials for lithium ion batteries. *Scientific Reports* 6:26146:1-10.

[28] Yagmurcukardes, M., Horzum, S., Torun, E., Nitrogenated, Peetersb, F. M., & Senger, T. R. (2016). Nitrogenated, phosphorated and arsenicated monolayer holey graphenes. *Physical Chemistry Chemical Physics* 18:3144-3150.

[29] Cooper, D. R., Anjou, B. D., Ghattamaneni, N., Harack, B., Hilke, M., Horth, A., Majlis, N., Massicotte, M., Vandsburger, L., Whiteway, E., & Yu, V. (2011). Experimental review of graphene, McGill University.

[30] Al-Muhit, B., & Sanchez, F. (2019). Tunable mechanical properties of graphene by clustered line pattern hydroxyl functionalization via molecular dynamics simulations. *Carbon* 146:680-700.

[31] Islam, Md. M., Faisal, S. N., Roy, A. K., Ansari, S., Cardillo, D., Konstaninov, K., & Haque, E. (2015). Synthesis of Nitrogen-Doped Graphene via Thermal Treatment of Graphene Oxide within Methylimidazole and its Capacitance Performance as Electric Double Layer Capacitor. *Journal of Nanotechnology and Materials Science* 2(2):1-5.

[32] R.S. Mulliken (1955). Mulliken populations. *Journal of Chemical Physics* 23, 1833-1841.

[33] Li, J., Liu, G., Long, X., Gao, G., & Wu, J. (2017). Different active sites in a bifunctional Co @ N-doped graphene shells based catalyst for the oxidative dehydrogenation and hydrogenation reactions. *Journal of Catalysis* 355:53-62.

[34] Li, J., Lin, L., Rui, D., Li, Q., Zhang, J., Kang, N., Zhang, Y., Pemg, H., Liu, Z., & Xu, H. Q. Electron-Hole Symmetry Breaking in Charge Transport in Nitrogen-Doped Graphene.

https://export.arxiv.org/ftp/arxiv/papers/1705/1705.01429.pdf

[35] Jalilian, R., Jauregui, L. A., Lopez, G., Tian, J., Roecker, C., Yazdanpanah, M. M., Cohn, R. W., Jovanovic I., & Chen, Y. P. (2011). Scanning gate microscopy on graphene: charge inhomogeneity and extrinsic doping. *Nanotechnology* 22:295705.

[36] Miyamoto, Y., Nakada, K., & Fujita, M. (1999). First-principles study of edge states of H-terminated graphitic ribbons. *Physical Review B* 59:9858.

[37] He, K., Lee, G. D., Robertson, A. W., Yoon, E., & Warner, J. H. (2014). Hydrogen-free graphene edges. *Nature Communications* 5:3040:1-7.

[38] Weinhold, F., Landi, C. R., & Glendening, E. D. (2016). What is NBO analysis and how is it useful? *International Reviews in Physical Chemistry* 35(3):399-440.